14. The CF occurs in the portion of the mid-IR spectrum where the real part of the complex refractive index is changing rapidly and approaching that of the surrounding medium, resulting in minimal scattering and an emissivity maximum.
15. Materials and methods are available as supporting material on *Science* Online.
16. P. D. Spudis, B. R. Hawke, P. Lucey, *J. Geophys. Res.* **89**, C197 (1984).
17. We defined a line using channels 3 and 5 and interpolated the value of the channel 4 emissivity on this line. We then subtracted the true channel-4 emissivity from this value.
18. M. Ohtake *et al*., *Nature* **461**, 236 (2009).
19. Diviner data meeting our analysis criteria have not been acquired over Mons La Hire, Darney Chi, or Darney Tau.
20. P. G. Lucey, G. J. Taylor, E. Malaret, *Science* **268**, 1150 (1995).
21. P. G. Lucey, D. T. Blewett, B. R. Hawke, *J. Geophys. Res.* **103**, 3679 (1998).
22. B. R. Hawke *et al*., *J. Geophys. Res.* **108**, 5069 (2003).
23. P. G. Lucey, B. R. Hawke, C. M. Pieters, J. W. Head, T. B. McCord, *J. Geophys. Res.* **91** (suppl.), D344 (1986).
24. B. B. Wilcox, P. G. Lucey, B. R. Hawke, *J. Geophys. Res.* **111**, E09001 (2006).
25. C. A. Wood, J. W. Head, *Conference on the Origin of Mare Basalts* (Lunar Science Institute, Houston, TX, 1975).
26. R. Wagner *et al*., *Lunar Planet. Sci.* **XXVII**, 1367 (abstract) (1996).
27. L. E. Nyquist, C. Y. Shih, *Geochim. Cosmochim. Acta* **56**, 2213 (1992).
28. B. L. Jolliff *et al*., *Am. Mineral.* **84**, 821 (1999).
29. C. R. Neal, L. A. Taylor, *Geochim. Cosmochim. Acta* **53**, 529 (1989).
30. B. L. Jolliff, *Int. Geol. Rev.* **40**, 916 (1998).
31. S. Maaløe, A. R. McBirney, *J. Volcanol. Geotherm. Res.* **76**, 111 (1997).
32. B. L. Jolliff, J. J. Gillis, L. A. Haskin, R. L. Korotev, M. A. Wieczorek, *J. Geophys. Res.* **105**, 4197 (2000).
33. D. J. Lawrence *et al*., *J. Geophys. Res.* **105**, 20307 (2000).
34. This work was funded in part by the Diviner science budget. T.D.G., J.L.B., M.B.W., and R.C.E. were supported by the NASA Lunar Reconnaissance Orbiter Participating Scientist program.

Supporting Online Material

www.sciencemag.org/cgi/content/full/329/5998/1510/DC1
Materials and Methods
Figs. S1 and S2
References

11 May 2010; accepted 1 September 2010
10.1126/science.1192148

Rainforest Aerosols as Biogenic Nuclei of Clouds and Precipitation in the Amazon

U. Pöschl,[1]* S. T. Martin,[2]* B. Sinha,[1] Q. Chen,[2] S. S. Gunthe,[1] J. A. Huffman,[1] S. Borrmann,[1] D. K. Farmer,[3] R. M. Garland,[1] G. Helas,[1] J. L. Jimenez,[3] S. M. King,[2] A. Manzi,[4] E. Mikhailov,[1,5] T. Pauliquevis,[6,7] M. D. Petters,[8,9] A. J. Prenni,[8] P. Roldin,[10] D. Rose,[1] J. Schneider,[1] H. Su,[1] S. R. Zorn,[1,2] P. Artaxo,[6] M. O. Andreae[1]

The Amazon is one of the few continental regions where atmospheric aerosol particles and their effects on climate are not dominated by anthropogenic sources. During the wet season, the ambient conditions approach those of the pristine pre-industrial era. We show that the fine submicrometer particles accounting for most cloud condensation nuclei are predominantly composed of secondary organic material formed by oxidation of gaseous biogenic precursors. Supermicrometer particles, which are relevant as ice nuclei, consist mostly of primary biological material directly released from rainforest biota. The Amazon Basin appears to be a biogeochemical reactor, in which the biosphere and atmospheric photochemistry produce nuclei for clouds and precipitation sustaining the hydrological cycle. The prevailing regime of aerosol-cloud interactions in this natural environment is distinctly different from polluted regions.

Atmospheric aerosols are key elements of the climate system. Depending on composition and abundance, aerosols can influence Earth's energy budget by scattering or absorbing radiation and can modify the characteristics of clouds and enhance or suppress precipitation. The direct and indirect aerosol effects on climate are among the largest uncertainties in the current understanding of regional and global environmental change. A crucial challenge is developing a quantitative understanding of the sources and properties of aerosol particles, including primary emission from the Earth's surface, secondary formation in the atmosphere, chemical composition and mixing state, and the ability to nucleate cloud droplets and ice crystals—all as influenced by human activities as compared with natural conditions (*1*–*4*).

During the wet season, the Amazon Basin is one of the few continental regions where aerosols can be studied under near-natural conditions (*5*–*7*). The Amazonian Aerosol Characterization Experiment 2008 (AMAZE-08) was conducted in the middle of the wet season at a remote site north of Manaus, Brazil (February to March 2008), and the investigated air masses came with the trade wind circulation from the northeast over some 1600 km of pristine tropical rainforest (*8*). Here, we focus on measurements performed in the period of 3 to 13 March 2008, when the influence of long-range transport from the Atlantic Ocean, Africa, or regional anthropogenic sources of pollution was particularly low and the aerosol properties were dominated by particles emitted or formed within the rainforest ecosystem (*6*, *7*, *9*, *10*). The measurement techniques applied include scanning electron microscopy (SEM) with energy-dispersive x-ray spectroscopy (EDX), atomic force microscopy (AFM), secondary ion mass spectrometry (NanoSIMS), aerosol mass spectrometry (AMS), differential mobility particle sizing (DMPS), ultraviolet aerodynamic particle sizing (UV-APS), and counting of cloud condensation nuclei (CCN) and ice nuclei (IN) (*8*). To our knowledge, this study provides the first comprehensive, detailed, and size-resolved account of the chemical composition, mixing state, CCN activity, and IN activity of particles in pristine rainforest air approximating pre-industrial conditions (*5*–*7*).

SEM images of characteristic particle types are shown in Fig. 1. Nearly all detected particles could be attributed to one of the following five categories: (i) secondary organic aerosol (SOA) droplets that were formed by atmospheric oxidation and gas-to-particle conversion of biogenic volatile organic compounds (*9*) and in which no other chemical components were detectable; (ii) SOA-inorganic particles composed of secondary organic material mixed with sulfates and/or chlorides from regional or marine sources (*6*); (iii) primary biological aerosol (PBA) particles, such as plant fragments or fungal spores (*6*, *11*, *12*); (iv) mineral dust particles consisting mostly of clay minerals from the Sahara desert (*6*, *13*); or (v) pyrogenic carbon particles that exhibited characteristic agglomerate structures and originated from regional or African sources of biomass burning or fossil fuel combustion (*6*). In mixed SOA-inorganic particles, the organic fraction was typically larger than the inorganic fraction. The primary biological, mineral dust, and pyrogenic carbon particles were also partially coated with organic material [supporting online material (SOM) text].

The average number and mass size distribution, composition, and mixing state of particles as detected with microscopy and complementary online measurements are shown in Fig. 2. The online instruments measure different types of equivalent diameters, which can vary depending on the shape and the density of the particles. Nevertheless, the size distribution patterns obtained with the different techniques are in overall agreement with each other. SEM is the one method that cov-

[1]Max Planck Institute for Chemistry, 55128 Mainz, Germany. [2]School of Engineering and Applied Sciences and Department of Earth and Planetary Sciences, Harvard University, Cambridge, MA 02138, USA. [3]Department of Chemistry and Biochemistry and Cooperative Institute for Research in Environmental Science, University of Colorado, Boulder, CO 80309, USA. [4]National Institute of Amazonian Research, 69060 Manaus, Brazil. [5]Atmospheric Physics Department, Institute of Physics, St. Petersburg State University, 198904 St. Petersburg, Russia. [6]Institute of Physics, University of São Paulo, 05508 São Paulo, Brazil. [7]Federal University of São Paulo, 04023 Diadema, Brazil. [8]Department of Atmospheric Science, Colorado State University, Fort Collins, CO 80523, USA. [9]Marine Earth and Atmospheric Science, North Carolina State University, Raleigh, NC 27695, USA. [10]Department of Physics, Lund University, 22100 Lund, Sweden.

*To whom correspondence should be addressed. E-mail: u.poschl@mpic.de (U.P.); scot_martin@harvard.edu (S.T.M.)

ers the full particle size range and provides detailed information about composition and mixing state. The online measurement techniques, however, are more reliable for the absolute concentration values because of their better sampling and counting statistics. The integral particle number and mass concentrations as well as the relative proportions of different types of particles corresponding to the displayed size distributions are summarized in tables S1 and S2. The observed particle number and mass size distributions can be separated into two characteristic fractions with a dividing diameter of 1 μm. The submicrometer fraction dominated the total particle number concentration (>99% of ~200 cm^{-3}) (Fig. 2A and table S1), whereas the supermicrometer fraction accounted for most of the total particle mass concentration (~70% of ~2 μg m^{-3}) (Fig. 2C and table S2).

The submicrometer fraction exhibited three characteristic modes as indicated by local maxima in the number size distribution (Fig. 2B): a nucleation mode (<0.03 μm), an Aitken mode (0.03 to 0.1 μm), and an accumulation mode (0.1 to 1 μm). According to single particle analysis (SEM, AFM, and NanoSIMS), pure SOA droplets dominated the nucleation and Aitken modes (number fraction >99%) (Fig. 2A). The accumulation mode consisted of pure SOA droplets, mixed SOA-inorganic particles, and pyrogenic carbon particles. Overall, the pure SOA droplets represented ~85% of the number concentration of submicrometer particles and potential CCN, and the mixed SOA-inorganic particles accounted for another ~10% (table S1).

The microscopy results were consistent with the accompanying online measurements. Specifically, the proportion of organic matter measured by AMS was >90% in the Aitken range and >80% in the accumulation range, in which the proportion of sulfate increased (Fig. 2D). The submicrometer organic mass concentrations determined by means of AMS were higher than the corresponding SEM results, which is probably due to partial evaporation (*14*). The average oxygen-to-carbon ratio of 0.44 and the mass spectra observed during AMAZE-08 for the submicrometer organic matter are in good agreement with laboratory studies of biogenic SOA from isoprene and terpene oxidation (*9*, *15*). PBA compounds detectable with AMS, such as proteins, amino acids, and carbohydrates, contributed less than 5% to the submicrometer particulate matter (*9*).

The predominance of SOA is further reflected in the effective hygroscopicity parameter κ determined through size-resolved CCN measurements (*10*). This parameter describes the influence of chemical composition on the ability of particles to absorb water vapor and form cloud droplets. Throughout the campaign, the κ values in the Aitken range were nearly constant at $\kappa \approx 0.1$, which is in agreement with laboratory investigations of biogenic SOA from isoprene and terpene oxidation (*4*, *16*) and much lower than the κ values of ammonium sulfate, sodium chloride, and other inorganic salts commonly observed in aerosols (0.6 to 1.3) (*17*). In the accumulation mode size range (0.1 to 1 μm), κ increased to ~0.15 as the proportion of sulfate increased to ~10% (Fig. 2D). Nevertheless, the effective hygroscopicity remained lower by a factor of approximately two than the approximate global continental average value of $\kappa \approx 0.3$ (*10*, *18*).

The supermicrometer fraction with a local maximum (coarse mode) around 2 to 3 μm consisted mostly of PBA particles with a number fraction of ~80% (mass fraction 85%) plus some mineral dust and mixed SOA-inorganic particles with number fractions of 10 and 6%, respectively (Fig. 2, A and C, and tables S1 and S2). The SEM results were consistent with online measurements of fluorescent biological aerosol (FBA) particles, which can be regarded as a lower-limit proxy for PBA particles (*19*, *20*). The number and mass fractions of supermicrometer FBA particles were 40 and 64%, respectively (Fig. 2, B and D, and tables S1 and S2).

Measurements and modeling of IN concentrations during AMAZE-08 suggest that ice formation in Amazon clouds at temperatures warmer than –25°C is dominated by PBA particles (*20*). Although the number concentration of such efficient biological IN is low (about 1 to 2 L^{-1}), they are nevertheless the first to initiate ice formation and can have a strong influence on the evolution of clouds and precipitation (*21*–*23*). At temperatures colder than –25°C, both locally emitted PBA and mineral dust particles imported from the Sahara desert can act as IN and induce cold rain formation. The IN activity of mineral dust may in fact also be influenced by biological materials, as suggested in earlier studies that include aircraft observations of ice cloud residuals (*21*, *24*). In any case, PBA particles appear to be the most efficient IN and, outside of Saharan dust episodes, also the most abundant IN in the Amazon Basin. Moreover, the supermicrometer particles can also act as "giant" CCN, generating

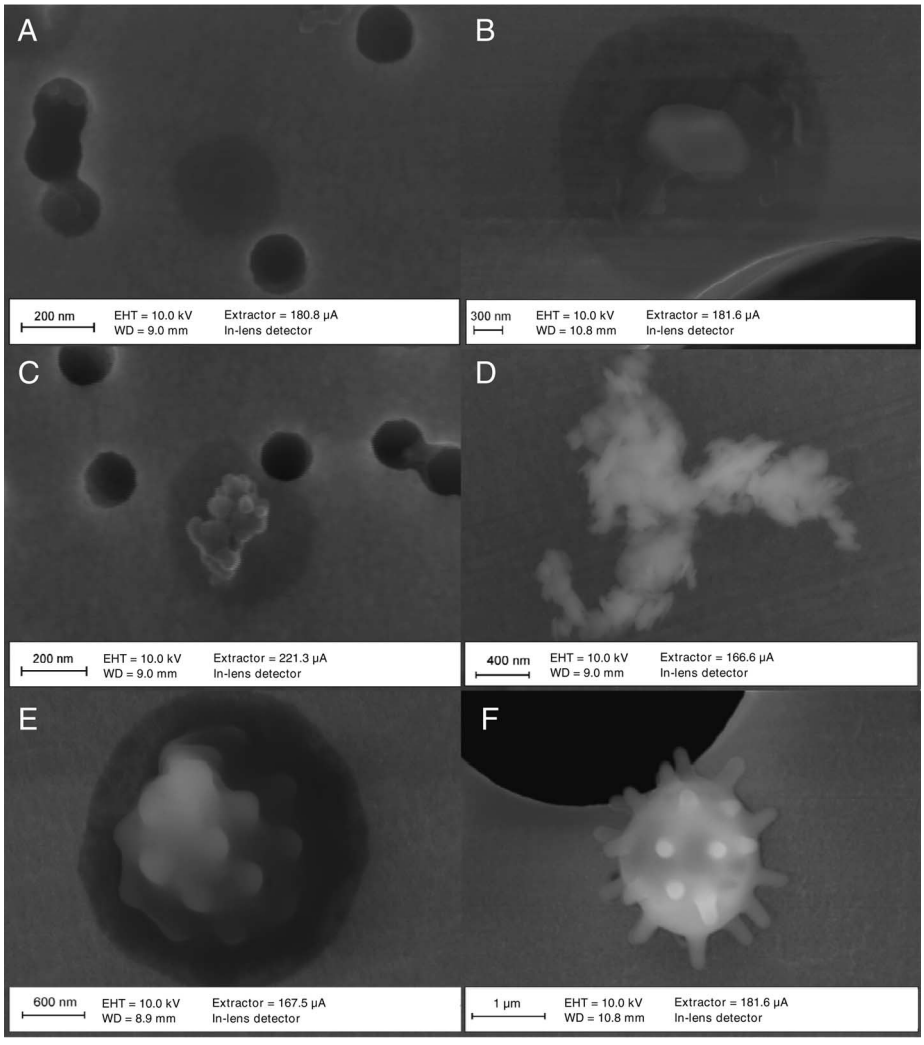

Fig. 1. Characteristic particle types observed by means of SEM of filter samples collected during AMAZE-08 (3 to 13 March 2008). (**A**) SOA droplet. (**B**) Mixed SOA-inorganic particle. (**C**) Pyrogenic carbon particle with organic coating. (**D**) Mineral dust particle without coating. (**E** and **F**) PBA particles (E) with and (F) without organic coating. SOA droplets and organic coatings appear dark gray, filter pores appear black, and filter material appears light gray (*8*).

large droplets and inducing warm rain without ice formation (*2*, *21*).

The low aerosol concentrations and the high proportions of secondary organic and primary biological matter suggest that the climate system interactions between aerosols, clouds, and precipitation over pristine rainforest regions may substantially differ from both pristine marine regions ("green ocean" versus "blue ocean") as well as from polluted environments (*2*, *25*). Model calculations using the aerosol size distributions and the hygroscopicity parameters determined in AMAZE-08 suggest that the activation of CCN in convective clouds over the pristine Amazonian rainforest is aerosol-limited, which means that the number of cloud droplets is directly proportional to the number of aerosol particles (fig. S1) (*26*). In contrast, the formation of cloud droplets in polluted environments (including parts of the Amazon Basin influenced by intense biomass burning during the dry season), tends to be updraft-limited, which means that the number of cloud droplets depends primarily on the updraft velocity (*26*). In these environments, the abundance of CCN is usually dominated by anthropogenic particles from sources related to combustion processes (*18*).

Over the pristine Amazonian rainforest, convective clouds for which biogenic SOA particles serve as CCN may in turn promote the formation of new SOA particles. During AMAZE-08, no new particle formation events were observed, which is consistent with earlier Amazonian aerosol studies (*6*, *7*) but unlike most other continental regions of the world (*27*, *28*). The low abundance of nucleation mode particles (<30 nm) (Fig. 2B, DMPS) and the relatively high abundance of SOA particles in the Aitken mode suggest, by inference, that new particle formation occurred in the free troposphere, possibly in the outflow of convective clouds, and that the newly formed particles were transported from aloft into the boundary layer, possibly in the downdraft of convective clouds (*6*, *7*, *29*, *30*). Similarly, precipitation induced by PBA particles acting as IN or giant CCN sustains the reproduction of plants and microorganisms in the ecosystem from which both the SOA precursors and the PBA particles are emitted (such as bacteria, fungi, pollen, and plant debris) (*6*, *11*). Accordingly, the Amazon Basin can be pictured as a biogeochemical reactor using the feedstock of plant and microbial emissions in combination with high water vapor, solar radiation, and photo-oxidant levels to produce SOA and PBA particles (*31*, *32*). The biogenic aerosol particles serve as nuclei for clouds and precipitation, sustaining the hydrological cycle and biological reproduction in the ecosystem (Fig. 3). The feedback mechanisms involved may be important for stabilizing the Amazonian rainforest ecosystem and may also be generally relevant for the evolution of ecosystems and climate on global scales and in the Earth's history. To test this hypothesis, we suggest further studies and long-term observations of aerosol properties and aerosol-cloud-precipitation interactions under pristine conditions in other regions and climatic zones with high biological activity, including tropical, temperate, and boreal forests.

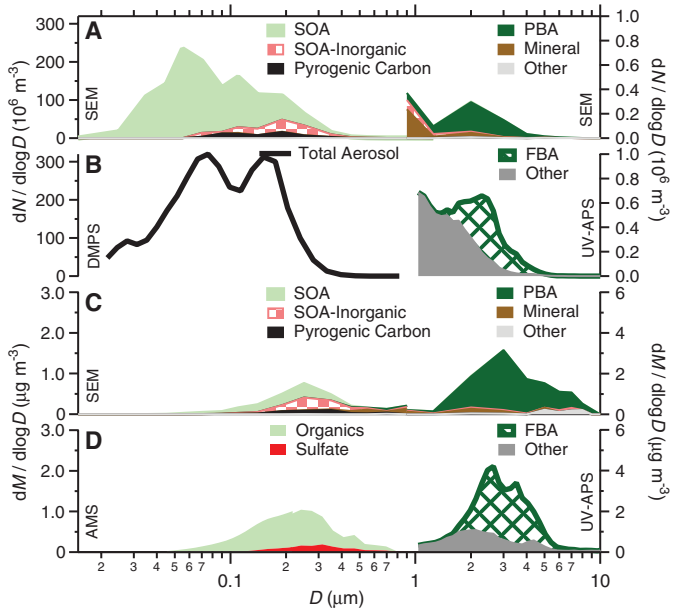

Fig. 2. Prevalence of different aerosol types in the (**A** and **B**) number size distribution (d*N*/dlog*D*) and (**C** and **D**) mass size distribution (d*M*/dlog*D*) plotted against particle diameter (*D*) as observed during AMAZE-08 (3 to 13 March 2008). Single particle analysis of filter samples was performed by means of SEM, and online measurements were made by means of differential mobility particle sizing (DMPS, <1 μm), aerosol mass spectrometry (AMS, < 1 μm), and ultraviolet aerodynamic particle sizing (UV-APS, >1 μm). Relative uncertainties are in the range of ~10 to 50% (*8*). There is a change of scales at D = 1 μm (left versus right ordinate).

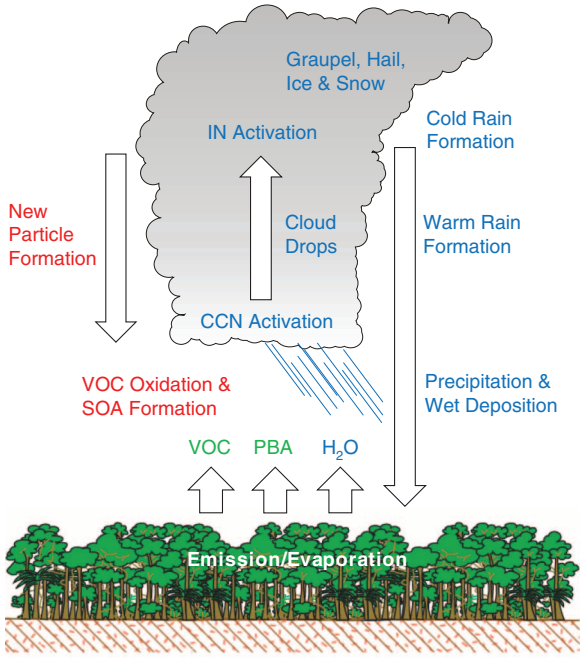

Fig. 3. Aerosol and water cycling over the pristine rainforest. SOA formed by photo-oxidation of volatile organic compounds (VOC) and PBA emitted from biota in the rainforest (plants and microorganisms) serve as biogenic nuclei for CCN and IN, which induce warm or cold rain formation, precipitation, and wet deposition of gases and particles.

References and Notes

1. S. Solomon *et al.*, *IPCC 4th Assessment Report* (Cambridge Univ. Press, Cambridge, 2007).
2. D. Rosenfeld *et al.*, *Science* **321**, 1309 (2008).
3. B. Stevens, G. Feingold, *Nature* **461**, 607 (2009).
4. J. L. Jimenez *et al.*, *Science* **326**, 1525 (2009).
5. M. O. Andreae, *Science* **315**, 50 (2007).
6. S. T. Martin *et al.*, *Rev. Geophys.* **48**, RG2002 (2010).
7. S. T. Martin *et al.*, *Atmos. Chem. Phys. Discuss.* **10**, 18139 (2010).
8. Materials and methods are available as supporting material on *Science* Online.
9. Q. Chen *et al.*, *Geophys. Res. Lett.* **36**, L20806 (2009).
10. S. S. Gunthe *et al.*, *Atmos. Chem. Phys.* **9**, 7551 (2009).
11. W. Elbert, P. E. Taylor, M. O. Andreae, U. Pöschl, *Atmos. Chem. Phys.* **7**, 4569 (2007).
12. J. Fröhlich-Nowoisky, D. A. Pickersgill, V. R. Després, U. Pöschl, *Proc. Natl. Acad. Sci. U.S.A.* **106**, 12814 (2009).
13. I. Koren *et al.*, *Environ. Res. Lett.* **1**, 014005 (2006).
14. K. S. Johnson *et al.*, *Environ. Sci. Technol.* **42**, 6619 (2008).
15. M. Hallquist *et al.*, *Atmos. Chem. Phys.* **9**, 5155 (2009).
16. S. M. King *et al.*, *Atmos. Chem. Phys.* **10**, 3953 (2010).
17. M. D. Petters, S. M. Kreidenweis, *Atmos. Chem. Phys.* **7**, 1961 (2007).
18. M. O. Andreae, D. Rosenfeld, *Earth Sci. Rev.* **89**, 13 (2008).
19. J. A. Huffman, B. Treutlein, U. Pöschl, *Atmos. Chem. Phys.* **10**, 3215 (2010).
20. A. J. Prenni *et al.*, *Nat. Geosci.* **2**, 402 (2009).

21. O. Möhler, P. J. DeMott, G. Vali, Z. Levin, *Biogeosciences* **4**, 1059 (2007).
22. B. C. Christner, C. E. Morris, C. M. Foreman, R. M. Cai, D. C. Sands, *Science* **319**, 1214 (2008).
23. R. M. Bowers *et al.*, *Appl. Environ. Microbiol.* **75**, 5121 (2009).
24. K. A. Pratt *et al.*, *Nat. Geosci.* **2**, 398 (2009).
25. M. O. Andreae *et al.*, *Science* **303**, 1337 (2004).
26. P. Reutter *et al.*, *Atmos. Chem. Phys.* **9**, 7067 (2009).
27. M. Kulmala *et al.*, *J. Aerosol Sci.* **35**, 143 (2004).
28. J. Merikanto, D. V. Spracklen, G. W. Mann, S. J. Pickering, K. S. Carslaw, *Atmos. Chem. Phys.* **9**, 8601 (2009).
29. R. Krejci *et al.*, *Atmos. Chem. Phys.* **5**, 1527 (2005).
30. A. M. L. Ekman *et al.*, *Geophys. Res. Lett.* **35**, L17810 (2008).
31. U. Kuhn *et al.*, *Atmos. Chem. Phys.* **7**, 2855 (2007).
32. J. Lelieveld *et al.*, *Nature* **452**, 737 (2008).

33. Support from a large number of colleagues, agencies, and institutions is gratefully acknowledged as detailed in the supporting online material.

Supporting Online Material
www.sciencemag.org/cgi/content/full/329/5998/1513/DC1
Materials and Methods
SOM Text
Fig. S1
Tables S1 to S6
References and Notes

19 April 2010; accepted 28 June 2010
10.1126/science.1191056

Melting of Peridotite to 140 Gigapascals

G. Fiquet,[1]* A. L. Auzende,[1] J. Siebert,[1] A. Corgne,[2,3] H. Bureau,[1] H. Ozawa,[1,4] G. Garbarino[5]

Interrogating physical processes that occur within the lowermost mantle is a key to understanding Earth's evolution and present-day inner composition. Among such processes, partial melting has been proposed to explain mantle regions with ultralow seismic velocities near the core-mantle boundary, but experimental validation at the appropriate temperature and pressure regimes remains challenging. Using laser-heated diamond anvil cells, we constructed the solidus curve of a natural fertile peridotite between 36 and 140 gigapascals. Melting at core-mantle boundary pressures occurs at 4180 ± 150 kelvin, which is a value that matches estimated mantle geotherms. Molten regions may therefore exist at the base of the present-day mantle. Melting phase relations and element partitioning data also show that these liquids could host many incompatible elements at the base of the mantle.

Geophysical and geochemical observations favor the presence of chemical heterogeneities in the lowermost mantle. These are thought to be either primitive mantle residues (*1*), dense subducted slab components (*2*), products of chemical interactions between the core and mantle (*3*, *4*), or dense melts perhaps as old as the Earth itself (*5*). The core-mantle boundary is a complex region that has been the focus of numerous geophysical studies. Seismologic studies suggest the presence of two large low-shear velocity provinces (LLSVPs) under the African continent and in the pacific basin (*6*, *7*). The consensus view is that these slow regions (which are possibly up to 1000 km thick) exhibit an anomalously low shear velocity and increased bulk modulus but are not usually thought to be partially molten (*8*). Additionally, extensively documented ultralow-velocity zones (ULVZs) correspond to localized features at the core mantle boundary (CMB), with strong reductions in seismic velocities (in the range of 10 to 30%) for both P and S waves (*9*, *10*); the interpretation is that these zones may be partially molten (*5*). Recent high-resolution waveform studies also find evidence that the ULVZ material is denser than the surrounding mantle (*11*). These partially molten regions have not been detected to be laterally continuous and have a thickness ranging from a few kilometers up to about 50 km.

It is attractive to link these observations with an episode of extensive melting that probably affected the primitive Earth, leading to the formation of a deep magma ocean. If the evolution of a terrestrial magma ocean resulted in the formation of a layer of melt at the base of the mantle early in Earth history, its survival depends on whether it was (and maybe still is) gravitationally and chemically stable (*12*). If this is the case, such a layer would be an ideal candidate for an unsampled geochemical reservoir hosting a variety of incompatible species, notably the planet's missing budget of heat-producing elements (*13*). The presence of high-pressure melts would also have consequences for chemical reactions between the mantle and core, the dynamics of the lowermost mantle, and the heat flow across the CMB.

To constrain the existence of melt at the base of the mantle, we performed melting experiments on a fertile peridotite composition over a range of lower-mantle pressures between 36 and 140 GPa using a laser-heated diamond-anvil cell (DAC) coupled with in situ synchrotron measurements (*14*). Our study thus extends the pressure range of previous measurements (*15*, *16*) of the solidus and liquidus temperatures of a mantle-like composition to depths exceeding those of the CMB at 2900 km. The starting material used for the high-pressure high-temperature melting experiments is a natural KLB-1 peridotite (*14*). To ensure chemical homogeneity at the smallest scale and Fe as mostly Fe^{2+}, a glass was prepared by using an aerodynamic levitation device coupled with CO_2 laser heating under slightly reducing conditions of oxygen fugacity (*17*). At high temperature, pressures were measured from cell parameters of the magnesium perovskite $(Mg,Fe)SiO_3$ by using a thermal equation of state recently reported for the same KLB-1 peridotitic starting material as

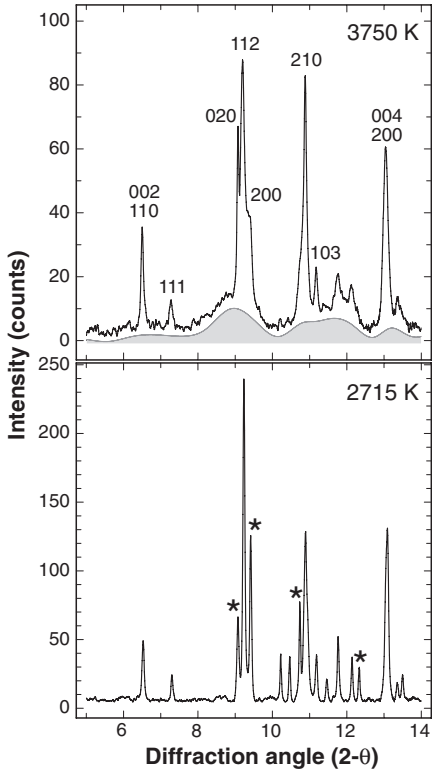

Fig. 1. Diffraction patterns collected at 61 GPa after normalized reference background subtraction: subsolidus at 2715 K (**bottom**) and above solidus at 3750 K (**top**). The diffuse scattering liquid contribution is outlined by the shaded area as a guide; it does not correspond to a physical structural model of the liquid. HKL indexes are given for remaining diffraction peaks that can be assigned to magnesium silicate perovskite, observed above the solidus temperature at this pressure (top). Stars denote diffraction peaks of Ca-perovskite and ferropericlase affected by partial melting at these conditions (bottom).

[1]Institut de Minéralogie et de Physique des Milieux Condensés, Institut de Physique du Globe de Paris, Université Pierre et Marie Curie, UMR CNRS 7590, Université Paris Diderot, 140 rue de Lourmel, 75015 Paris, France. [2]Institut de Physique du Globe de Paris, Equipe de Minéralogie à l'Institut de Minéralogie et de Physique des Milieux Condensés, 140 rue de Lourmel, 75015 Paris, France. [3]Observatoire Midi-Pyrénées, UMR CNRS 5562, 14 rue Edouard Belin, 31400 Toulouse, France. [4]Department of Earth and Planetary Sciences, Tokyo Institute of Technology 2-12-1 Ookayama, Meguro-ku, Tokyo 152-8551, Japan. [5]European Synchrotron Radiation Facility, BP220, 38043 Grenoble cedex, France.

*To whom correspondence should be addressed. E-mail: guillame.fiquet@impmc.upmc.fr

Science

Rainforest Aerosols as Biogenic Nuclei of Clouds and Precipitation in the Amazon

U. Pöschl, S. T. Martin, B. Sinha, Q. Chen, S. S. Gunthe, J. A. Huffman, S. Borrmann, D. K. Farmer, R. M. Garland, G. Helas, J. L. Jimenez, S. M. King, A. Manzi, E. Mikhailov, T. Pauliquevis, M. D. Petters, A. J. Prenni, P. Roldin, D. Rose, J. Schneider, H. Su, S. R. Zorn, P. Artaxo and M. O. Andreae

Science **329** (5998), 1513-1516.
DOI: 10.1126/science.1191056

Clean or Dirty

Aerosols strongly affect atmospheric properties and processes—including visibility, cloud formation, and radiative behavior. Knowing their effects in both clean and polluted air is necessary in order to understand their influence (see the Perspective by **Baltensperger**). **Clarke and Kapustin** (p. 1488) examine vertical atmospheric profiles collected above the Pacific Ocean, where air quality is affected by the transport of polluted air from the west, and find significant regional enhancements in light scattering, aerosol mass, and aerosol number associated with combustion. Aerosol particle concentrations in this region can exceed values in clean, unperturbed regions by over an order of magnitude. Thus combustion affects hemispheric aerosol optical depth and the distribution of cloud condensation nuclei. **Pöschl *et al.*** (p. 1513) discuss the composition of aerosols above the Amazon Basin, in the pristine conditions of the rainy season. The aerosols in this region are derived mostly from gaseous biogenic precursors, plants, and microorganisms, and particle concentration is orders of magnitude lower than in polluted continental regions.